Journal of Polymers and the Environment (2021) 29:2310–2320
https://doi.org/10.1007/s10924-020-02017-x

ORIGINAL PAPER

The Soil Biodegradability of Structured Composites Based on Cellulose Cardboard and Blends of Polylactic Acid and Polyhydroxybutyrate

Elena-Ruxandra Radu[1] · Denis Mihaela Panaitescu[1] · Cristian-Andi Nicolae[1] · Raluca Augusta Gabor[1] · Valentin Rădiţoiu[1] · Sergiu Stoian[1] · Elvira Alexandrescu[1] · Radu Fierăscu[1] · Ioana Chiulan[1]

Accepted: 15 December 2020 / Published online: 20 January 2021

Abstract

The excessive use of plastics, in addition to the limitative capacities available for plastic waste disposal or recycle increased the interest in degradable polymers. Polylactic acid (PLA) and polyhydroxybutyrate (PHB) are among the most studied biobased polymers for packaging applications. However, their biodegradability in real environment is questionable. Therefore, the purpose of this study was to investigate the biodegradation behavior of PLA/PHB blend films and their sandwich-structured composites containing a cellulose paper interlayer, in natural soil environment, exposed to humidity and temperature conditions specific to different seasons. The study was conducted for 8 months and the biodegradation process was evaluated by measuring the morphological changes, weight loss and tensile properties of the samples. The weight loss data showed that materials were able to degrade under the action of soil microorganisms, water and heat. Moreover, the cellulose layer favored the water retention and enhanced the degradation. SEM images highlighted traces of erosion and biodegradation in the case of the buried samples and FTIR spectra revealed the scission of the ester bonds, which proved the degradation of the aliphatic polyesters. The XRD studies showed that the samples recovered from compost soil were more crystalline than those stored at room temperature, which indicates the degradation of the amorphous phase in the samples. In addition, DMA measurements showed a strong reinforcing effect of the cellulose interlayer on the PLA/PHB matrix. In conclusion, PLA/PHB blend is suitable for long packaging application, but the addition of a cellulose paper interlayer is beneficial to accelerate the decomposition rate.

Keywords Soil biodegradability · Polylactic acid · Polyhydroxybutyrate · Packaging

Introduction

In the last decade, the plastic-based food packaging industry has constantly increased. Unfortunately, environmental pollution is the downside of the non-biodegradability character of plastic-based packaging, with a low recycling rate, of less than 3% worldwide [1]. Efforts are being made to develop eco-friendly packaging to reduce the harmful effects of petroleum-based polymers [2]. The solution is to reduce the plastics waste by replacing synthetic polymers with biodegradable ones [3]. Biodegradable polymers are a class of polymers that decompose, in a relatively short time, under the action of microorganisms, such as fungi and bacteria [4]. The most studied biopolymers for developing environmentally friendly and biodegradable food packages are chitosan, starch, polyvinyl alcohol, cellulose, polyhydroxybutyrate (PHB) and polylactic acid (PLA) [5, 6]. PLA is a noticing real-world example of substitutes for a large variety of plastic-based products, which burdens the terrestrial and aquatic ecosystems. Polylactic acid is becoming progressively more used in food-packaging industry, due to its high mechanical strength, transparency, processability, non-toxicity, biodegradability and sustainability [7].

The major drawbacks of PLA are poor gas-barrier properties, reduced thermal stability, inherent brittleness, low toughness and poor ductility [8, 9]. Disadvantages like slow degradation rate and high cost limits its extensive application [10]. The incorporation of reinforcements, such as cellulose [11] or nanoclays [12, 13] has been found to improve its thermal stability and mechanical strength along with a

✉ Ioana Chiulan
ioana.chiulan@yahoo.com

[1] Polymer Department, National Research and Development Institute for Chemistry and Petrochemistry-ICECHIM, 202 Spl. Independentei, 060021 Bucharest, Romania

supplementary cost reduction. Alternatively, to increase the toughness of PLA some polymers were used, such as poly(butylene adipate-co-terephthalate), polyurethane, polyamide elastomer, starch or PHB [14]. PHB is a biodegradable thermoplastic polyester, with high crystallinity (50–80%), excellent gas barrier properties and mechanical properties similar to those of polypropylene [7, 15]. PLA and PHB present similar melting temperature and therefore can be processed in the melt state in blends of different compositions. It has been found in previous studies that the best synergetic effect is achieved for a PLA/PHB ratio of 75/25 (wt%) [16, 17]. The PHB crystals increase the crystallinity of PLA, while PLA improves the stiffness of PHB. However, PHB delays the PLA disintegration under composting [18].

Numerous variables are involved in the soil degradation of PLA, such as the material formulation, crystallinity, molecular weight, processing parameters [19]. Under normal conditions, PLA is stable, but degrades in environments of high temperature, humidity and bacterial activity, through a hydrolysis mechanism. Thus, the high-molecular-weight polyester chains are reduced to lower-molecular-weight oligomers. Eventually, these smaller molecules are completely converted in CO_2, H_2O and humus, under the influence of microorganisms in the environment they end up in [20]. The compost conditions are very different from soil environment, and consequently significant differences in the PLA's biodegradation rate occur. The PLA is hydrolyzed into smaller molecules (oligomers, dimers, and monomers) after composting at a temperature of 50–60 °C for 45–60 days [8, 20]. However, its degradation is very slow at temperatures below its glass transition and in low humidity [21]. The biodegradation process accelerates under acidic or basic conditions and is highly affected by both temperature and moisture levels. The degradation of PLA has been already studied in different environments, at laboratory scale using enzymes and cell cultures or directly in the complex conditions of natural landfills [22, 23].

PLA is non-degradable in water [24, 25] and slowly degradable in soil probably because of reduced temperature, water content and microbial activity. Bio-stimulation and bio-augmentation strategies involve the addition of fungal and bacterial strains to enhance the mineralization of PLA and studies carried out at ambient temperature were recently reported [26]. The biodegradation rate of PLA was accelerated by the incorporation of TiO_2 nanoparticles [27], montmorillonite [28], surfactants [29] or cellulose [30].

Cellulose cardboard is largely distributed in the consumer market, in the form of paper bags, boxes, packaging, hygiene products, and different commodities. Cyras et al. obtained bilayer composites made of cellulose cardboard and PHB, with barrier and mechanical properties suitable for packaging applications [31]. A critical demand in food packaging is to control the changes in the material's properties in humid environment and to predict the interactions between water or low molecular weight substances and polymer. Industrial composting conditions are carried out usually at high temperature (above 50 °C) and high relative humidity. However, a significant quantity of disposable bags or food packaging ends up in landfills, especially in the rural areas, where variable temperature and humidity conditions are encountered. There is clearly a lack of information on the mechanisms involved in the degradation process of PLA blends or composites in landfills with temperate-continental climate, with an annual average temperature of 8–11 °C. Therefore, the changes that occur in the properties of the materials intended to replace the common plastic-based packaging needs to be investigated in real environment.

The aim of this work was to study the soil biodegradation process of a PLA/PHB film and its sandwich-structured composite with cellulose paper, and to assess the impact on the morphological, mechanical and thermal properties. The study is focused on soil burial degradation behavior of sandwich-structured composites obtained by pressing, with the following composition: (i) two outer layers made of PLA/PHB films and (ii) an intercalated layer of cellulose paper treated superficially via silanization. The potential of the obtained sandwich-structured composite to be used in food-packaging applications, such as Tetrapak, was assessed.

Experimental Part

Materials

Polylactic acid used in this study was of 4032D type from Nature Works LLC, USA, and consisted of 1.4% D-Lactide units ($M_n \sim 150{,}000$ Da). This biopolymer is accepted by the Food & Drug Administration (FDA) to be used in food packaging materials. Powdered polyhydroxybutyrate (PHB) ($Mw = 4.9 \times 10^5$ g/mol, density 1.25 g/cm^3) was supplied by Biomer, Germany. Commercial cellulose cardboard with a thickness of 0.078 mm was provided by a local company.

Samples Preparations

PLA/PHB Blend

Prior to melt compounding, PLA and PHB polymers were dried in a ventilated oven at 50 °C for 3 h. The PLA/PHB polymer blends with a weight ratio of 75/25 were obtained using a Brabender Plastograph LabStation (Germany), with a mixing cell of 30 cm^3, under the following conditions: temperature 170 ± 5 °C, mixing for 7 min, and rotor speed of 60 rpm. The blends were further processed on a two-roll mill heated at 80 °C and compressed into sheets using an electrically heated press P200E (Dr. Collin,

Germany), under the following conditions: (i) preheating: 170 °C, 120 s, 5 bar; (ii) pressing: 170 °C, 60 s, 100 bar; (iii) cooling: 75 °C, 60 s, 5 bar. The sample was denoted PLA/PHB/0.

Silanization of Cellulose Paper

The surface of cellulose paper was treated by silanization for a better adhesion with the PLA/PHB matrix. The reaction was performed by immersing the paper in a mixture of water/ethanol (10/90, wt%), over which 10% aminopropyltriethoxysilane (relative to water) was added. The surface silanization was allowed to proceed for 3 h, at ambient temperature. Afterwards, the surface treated cellulose paper was dried into a ventilated oven, at 110 °C, for 2 h.

Sandwich-Structured Composite

The sandwich-structured composite (sample PLA/PHB/S/0) was prepared via compression molding on a laboratory heating press P200E (Dr. Collin, Germany), at 169 °C with 150 s of preheating at 5 bar and 50 s of compression at 10 bar. The silanized paper was pressed between the two PLA/PHB sheets, with an individual thickness of 0.035 mm.

Characterization

Biodegradability Assessment Using Soil Burial Test

The composting studies were performed outdoors, for 8 months, following a method described by Wei et al. [32], with some modifications. The blend film and the sandwich structured composite were cut in specimens with the size of 40 mm × 10 mm and dried in a vacuum oven at 50 °C until a constant weight. Five replicates for each sample were placed in a plastic box in a mixture of manure, flower and sand soil, in equal parts, and left on the windowsill. The soil was kept moist with water every 2–3 days. After 8 months, the specimens were removed from the ground, brushed softly, washed with water and dried in vacuum until constant weight. The samples removed from the compost were denoted as PLA/PHB/8 and PLA/PHB/S/8, respectively.

The film weight retention was determined using the following equation:

$$R_f = \frac{m}{m_0} * 100\% \quad (1)$$

where, R_f is the film weight retention after degradation via soil burial test, m is the film weight after degradation test, and m_0 is the initial weight of the film.

Thermal Characterization

Thermogravimetric analysis (TGA) was carried out using TGA Q5000 analyzer V3.13 (TA Instruments, USA). The samples (6–8 mg placed in aluminum pans) were heated from 25 to 700 °C, at a heating rate of 10 °C/min, using nitrogen as purge gas (40 mL/min). Experiments were performed in duplicate.

Differential scanning calorimetry (DSC) measurements were carried out on a DSC Q2000 V24.9 from TA Instruments (USA) operating under helium flow (25 mL/min). Samples of around 5 mg were tested with a heating/cooling rate of 10 °C/min as follows: cooling from 30 to − 50 °C, heating from − 50 to 200 °C, isothermal for 2 min in order to erase the thermal history and subsequent cooling to − 50 °C, held for 2 min and reheated to 200 °C. The glass transition temperature (T_g) was taken at the midpoint at half height of the heat capacity changes. The melting temperature (T_m), the cold crystallization temperature (T_{cc}) and their corresponding enthalpies (ΔH_m, ΔH_{cc}) were obtained from the first heating.

Dynamic Mechanical Analysis (DMA)

The thermo-mechanical analysis of the samples was carried out on a DMA Q800 V20.24 instrument, in tensile mode, at a frequency of 1 Hz. Samples were cut into 13 × 7 × 0.3 mm strips and measured in the temperature range from − 42 to 140 °C at a heating rate of 3 °C/min.

Surface Chemistry Characterized by FTIR Spectroscopy

Fourier transformed infrared (FTIR) measurements of the blend and sandwich-structured composite were obtained using a Jasco FTIR 6300 spectrophotometer (Jasco Co., Tokyo, Japan), and equipped with a Golden Gate ATR (diamond crystal) from Specac Ltd., London, UK. The spectra were recorded in the range of 4000–400 cm^{-1}, with 30 scans and 4 cm^{-1} resolution.

Morphology

The morphology of the soil exposed samples was evaluated using scanning electron microscopy (SEM) method and the images were obtained on an ESEM-FEI Quanta 200, Eindhoven (Netherlands) instrument.

X-ray Diffraction (XRD)

XRD analysis was performed on a X-ray diffractometer (Rigaku Corporation, Japan) with a Cu Kα (λ = 0.1541 nm) source, at 2θ values of 5–90°, with a scanning rate of 8°/min. The accelerating voltage of the generator radiation was set

at 45 kV and the emission current at 200 mA. The crystallinity index was calculated by dividing the area under the crystalline peaks by the total area (under the crystalline and amorphous peaks). The inter-planar distances were calculated by using Bragg's law, according to Eq. 2:

$$d = \frac{\lambda}{2sin\theta} \quad (2)$$

where λ is the wavelength and θ is the diffraction angle.

Crystal dimension (D_{hkl}) was determined using Scherrer's equation:

$$D_{hkl} = \frac{0.9 * \lambda}{\beta * cos\theta} \quad (3)$$

where β is the peak width at half maximum (in radians).

Results and Discussions

Visual and Morphological Characterization After Soil Biodegradation

The visual inspection showed a slight darkening of the PLA/PHB blend after soil burial, and a consistent disintegration of the intermediate layer of cellulose cardboard, indicating that cellulose fibers are more prone to biodegradation than the blend of the selected bioplastics (Fig. 1). It was clearly seen a loss of luster and the formation of small and dense pits, which demonstrate that PLA/PHB blend experienced both surface and bulk degradation during testing. However, a consistent decomposition of the bioplastic film or detaching the polymer layers from the silanized paper was not noticed. The samples buried in moist active soil, were adequately cleaned and dried, to give a precise weight loss. Table 1 shows the gravimetric values of the samples before and after the biodegradation tests in the soil, respectively. The results show a reduction of the sample mass by 14 and 16% under the action of soil microorganisms, water and heat, the sandwich-structured composite having the highest weight loss. Previous studies reported that the soil biodegradation rate is significantly accelerated when PHB was compounded with potato peel waste fermentation residue fibers, especially when the fiber content was higher than 15% [32]. PLA formulations require special conditions to degrade in times compatible with current waste management strategies. The biodegradation of PLA can be triggered by the addition of additives, microcrystalline cellulose [23, 33], lignocellulosic materials, such as paddy straw [34] or biopolymers (chitosan, gelatinized starches) [8, 35]. This effect was explained either by the dissolution of the soluble additives or the leaching of highly degradable components,

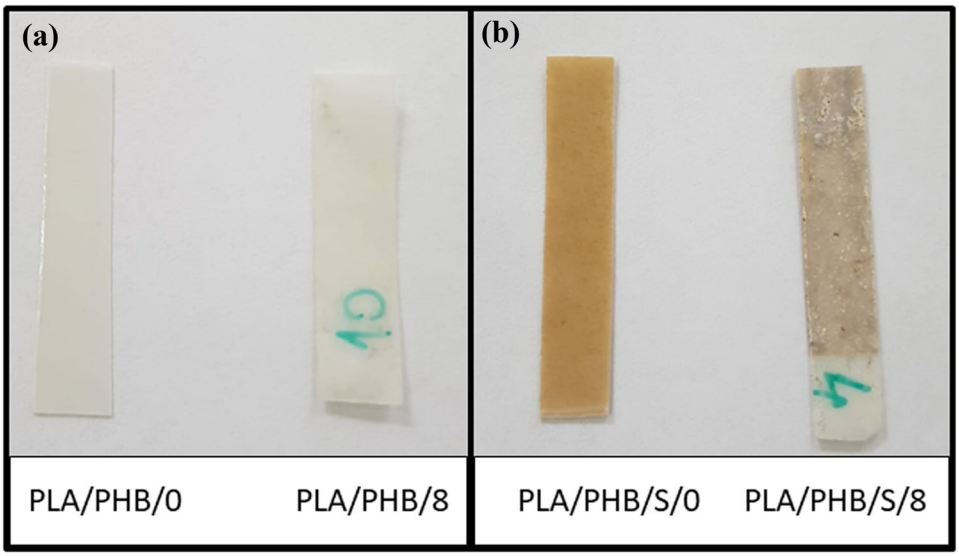

Fig. 1 Samples before and after 8 months in the soil: PLA/PHB blend (**a**) and PLA/PHB/S sandwich-structured composites (**b**)

Table 1 Evaluation of samples weight loss

Sample	Weight before soil burial test (g)	Weight after soil burial test (g)	Film weight retention (%)	Standard deviation
PLA/PHB	0.124	0.1064	85.78	4.08
PLA/PHB/S	0.1561	0.1311	83.98	4.06

creating pores, voids and cracks on the polymer surface. Finally, this facilitates the attack of the microorganisms during composting, resulting in a weight loss. In our case, the water was absorbed and retained by the intermediate cellulose paper and the two polymeric layers were exposed to a continuous humid environment. That's why the weight loss of the sandwich-structured composite was higher than that of the PLA/PHB film.

The SEM images of the PLA/PHB blend and PLA/PHB/S sandwich surfaces, before and after 8 months of soil burial degradation are shown in Fig. 2.

The SEM images of the samples exposed to the soil biodegradation test show traces of erosion and biodegradation. Before the biodegradation test, the surface of both PLA/PHB (Fig. 2a) and PLA/PHB/S (Fig. 2c) has a smooth appearance, without unevenness. After biodegradation test, the surface morphology changes, becoming rough, with traces of erosion, but without the disintegration of PLA/PHB (Fig. 2b) and PLA/PHB/S (Fig. 2d) samples. The increase of the surface roughness of PLA and PHB films after exposure to soil biodegradation has been reported in the literature [16, 36, 37]. These observations can be correlated with the gravimetric results, where a weight loss was observed, highlighting biodegradation. In addition, visible ruptures and consistent changes in physical appearance of the cellulose layer were noticed (data not shown).

XRD Analysis

The PLA/PHB blend and the structured composite were characterized by X-ray diffraction to study the effect of the compost soil and weathering conditions on the crystal structure and crystallinity. It is generally accepted that the degradation of PHA and PLA under burial composting conditions starts with the amorphous regions [38], but neighboring crystal regions may be also affected. Therefore, XRD is a useful technique to estimate the degree of disintegration of the plastic at the end of the test. The diffraction peaks characteristic for PLA are less visible in the diffractograms, because PLA exhibits a lower crystal growth rate and crystallinity than PHB [16, 39]. In Fig. 3 the XRD patterns of all samples showed the characteristic peaks of PHB, PLA, cellulose and some additional peaks, at $2\theta = 9.4°$, 18.8° and 28.5°, assigned to the inorganic filler (talc), present in PHB [40]. The crystalline peaks of PHB, the minor component in the blend, appeared at $2\theta = 13.4°$, 20°, 21.4°, 22.6°, 25.4°, 26.8° and 30.5°. The interplanar distances (d_{hkl}), the Miller indices (h, k and l) corresponding to each Bragg angle, the

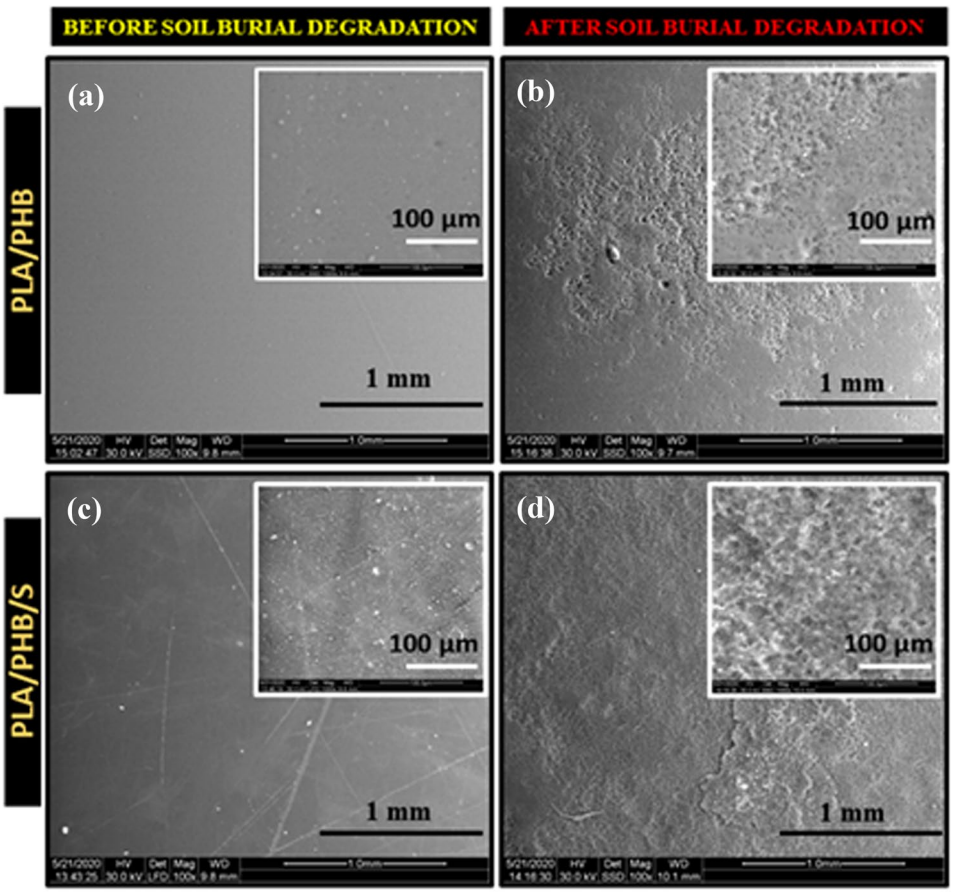

Fig. 2 SEM images for PLA/PHB blends before (**a**) and after (**b**) soil burial degradation and PLA/PHB/S before (**c**) and after (**d**) soil burial degradation

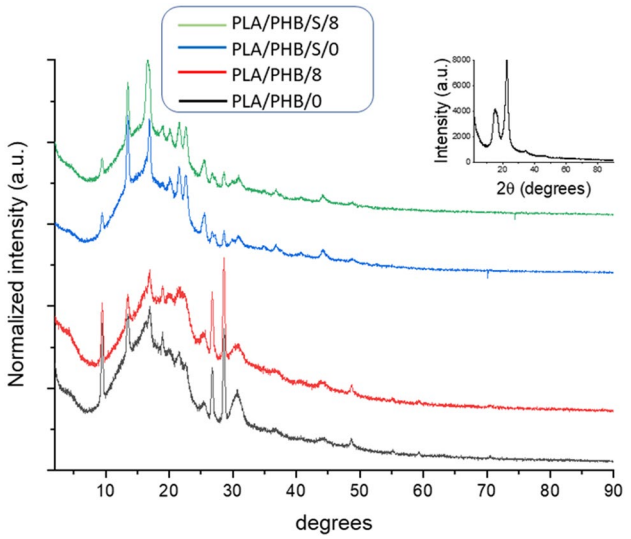

Fig. 3 XRD patterns of the samples before and after composting (inset: X-ray diffractogram of the cellulose paper)

crystallites sizes perpendicular to the 200 plane (D_{200}) and crystallinity indices for blends and composites are given in Table 2.

The interplanar distances are smaller in the structured composite compared to the plain blend and this tendency is further observed after soil burial showing the effect of supplementary compression processing and soil erosion. In addition, the apparent crystal size (D_{200}) was smaller in the structured composites than in the blend and also smaller after soil burial. This is also an effect of the supplementary processing and moist active soil, which may decrease the molecular weight of surface PHB [41]. The values recorded for the full-width at half maximum of the peak (β) were higher for the structured composite compared with the blend. Additionally, higher β values were obtained in the case of the buried samples as compared to the original samples kept in desiccator. This suggests a lower organization of the crystalline phase after the fabrication process of sandwich-structured composite and after the soil burial test.

The higher crystallinity index values obtained for the composted samples indicate the degradation of the amorphous phase, which is firstly attacked [38]. This is not necessarily correlated with a better organization of the crystalline phase and higher crystal dimensions. In fact, it can be seen from Fig. 3 that the main diffraction peaks become less sharp after soil burial test, which suggests that the ordering level of PHB molecular chains diminished. Several studies have found that the crystallinity of PLA and PHA-based composites increased after biodegradation [34, 38], because during the initial stages of degradation only amorphous regions were consumed.

FTIR Analysis

The IR spectra were recorded to examine the impact of soil conditioning on the chemical structure of the PLA/PHB blends and their sandwiches (Fig. 4). It can be seen that the soil burial test carried out over a period of 8 months brought significant changes in the FTIR spectra for both samples. The bands detected at 2995 cm^{-1} and 2942 cm^{-1} shows the –CH stretching characteristic to PLA [42]. The peak at 1750 cm^{-1} shows the typical stretching of amorphous

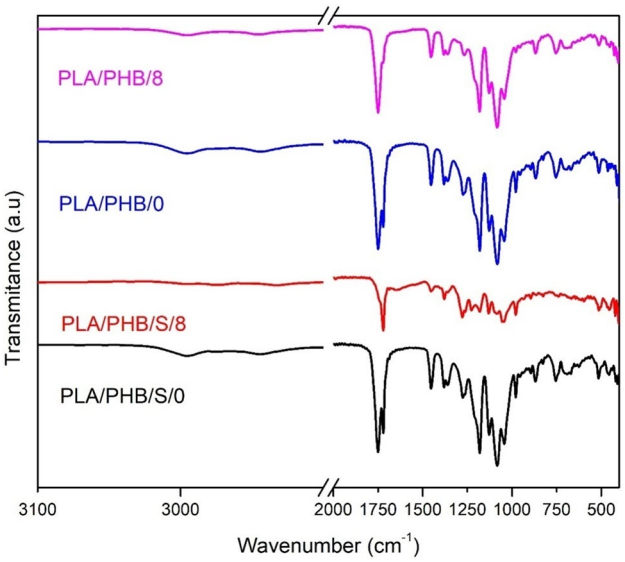

Fig. 4 FT-IR spectra for PLA/PHB blend and PLA/PHB/S sandwich-structured composite, before and after soil burial test

Table 2 XRD interplanar distances (d_{hkl}), crystallites size (D_{hkl}) and crystallinity indexes (C) for the samples before and after soil degradation

Sample	2θ ≈ 13.4 d_{020} (nm)	2θ ≈ 16.8 d_{110} (nm)	2θ ≈ 20.0 d_{021} (nm)	2θ ≈ 21.5 d_{101} (nm)	2θ ≈ 22.6 d_{111} (nm)	2θ ≈ 25.4 d121 (nm)	2θ ≈ 26.8 d_{040} (nm)	2θ ≈ 30.5 d_{200} (nm)	D_{200} (nm)	C (%)
PLA/PHB/0	0.6607	0.5497	0.4450	0.4136	0.3936	0.3507	0.3321	0.2922	12.54	19.9
PLA/PHB/8	0.6562	0.5220	0.4428	0.4117	0.3978	0.3505	0.3329	0.2953	9.96	34.8
PLA/PHB/S/0	0.6607	0.5276	0.4413	0.4120	0.3921	0.3495	0.3321	0.2883	10.20	21.9
PLA/PHB/S/8	0.6565	0.5329	0.4394	0.4120	0.3921	0.3484	0.3331	0.2907	6.58	32.7

carbonyl group (C=O) attributed to lactide [43]. All these peaks were clearly observed in PLA/PHB blend and structured composite before composting (Fig. 4). However, these absorption peaks were not distinguishable in the spectrum of PLA/PHB/S/8, which suggests the scission of ester bonds. Fukushima et al. reported that the degradation of linear aliphatic polyesters takes place through the scission of ester bonds, by enzymatically catalyzed hydrolysis, due to the presence of microorganisms in the soil [44].

Furthermore, the band at around 1720 cm^{-1}, present in the spectra of PLA/PHB and PLA/PHB/S before the soil burial test, and associated with crystalline C=O stretching vibration of PHB [45], is barely noticeable in the spectrum of both degraded samples. A new band appears at 1656 cm^{-1} in the spectrum of PLA/PHB/S sample; it has been previously observed during the degradation of PLA-MCC composite and correlated with the presence of carboxylate ions in degraded PLA composites [33, 46]. This chemical change is due to the microorganisms present in soil which consume lactic acid and its oligomers from the surface and leave carboxylate ions at the chain end [47]. The peak at 1450 cm^{-1} is assigned to the lactides $–CH_3$ group and its intensity is decreased after composting. The –C–O– bond stretching in –CH–O– group of PLA appeared at 1181 cm^{-1} [33] and shows a drastic decrease in intensity after the degradation tests.

Overall, the FT-IR spectra showed that after the soil burial test, the obtained composites displayed significant changes in the characteristic peaks. This indicates the degradation of the polymer layer, which is also confirmed by the weight loss analysis.

Thermogravimetric Analysis

The thermal stability of the blend and composite, before and after soil biodegradation test was evaluated through TGA. The weight loss curves and corresponding derivatives are shown in Fig. 5, and the main parameters are summarized in Table 3. The temperature corresponding to the onset of decomposition (T_{onset}) is essential for evaluating the thermal stability of the samples. It is noteworthy that the degradation curves for all the samples present similar profile, slightly different in the case of the composted sandwich. The degradation of PLA/PHB occurred in two steps, while the PLA/PHB/S sample presents a supplementary event of weight loss at around 350 °C and attributed to cellulose pyrolysis. The first weight loss starts at around 230 °C up to 280 °C and corresponds to PHB degradation, as reported previously [48]. The second and most important weight loss is noticed between 300 and 380 °C and is attributed to the decomposition of PLA, the major component of the polymer matrix. These values are in agreement with results reported for PLA [18, 49, 50]. As expected, the control sample, PLA/PHB/0,

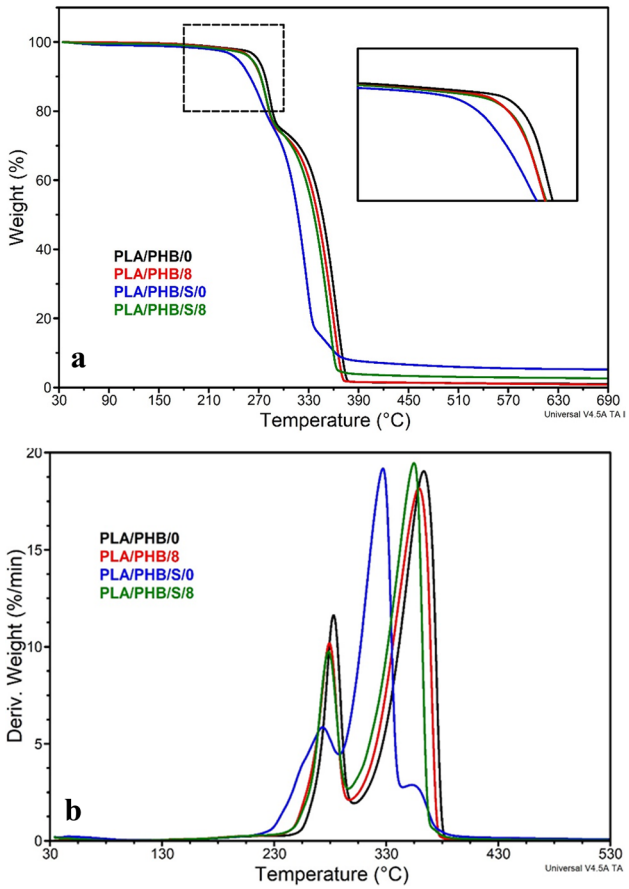

Fig. 5 TGA (**a**) and DTG (**b**) curves of the blend (PLA/PHB) and the structured composite (PLA/PHB/S) before and after soil burial test

was more thermally stable than composted samples and, to a greater extent than the structured-composite before soil burial. This suggests that water and other degradation products of cellulose favor the degradation of PHB which begin to decompose at a lower temperature. The water adsorption was found to accelerate the hydrolysis of PHB and this effect was even more pronounced when hydrophilic additives were added [51, 52]. This behavior was also observed in vivo, in the case of PHB particles loaded with a hydrophilic drug, whose dissolution created pores, increasing the water uptake and accelerating the polymer degradation by hydrolytic scission [52]. However, the T_{onset} of the composted sandwich was higher (Table 3), probably because of the consistent degradation of the outer layer after 8 months, as observed visually and in the SEM images (Fig. 2) and the consumption of lactic acid and its oligomers, as highlighted by FTIR. This reduced their contribution to the sample's composition and on the onset degradation temperature. The highest shift of the main degradation step was observed for PLA/PHB/S/0 sample, as shown by the derivatives curves (Fig. 5). Its reduced thermal stability is attributed to the presence of cellulose interlayer, phenomenon observed in the case of some

Table 3 TGA parameters (T_{onset}—the temperature at which the weight loss begins, $T_{5\%}$—temperature corresponding to 5% weight loss, T_P—the temperature of the maximum weight loss rate and the residue at 700 °C)

Sample	T_{onset} (°C)		$T_{5\%}$ (°C)	T_P (°C)			Residue at 700 °C (%)
	Peak 1	Peak 2		Peak 1	Peak 2	Peak 3	
PLA/PHB/0	270.2	336.7	269.1	283.3	363.8	–	1.03
PLA/PHB/8	264.7	332.6	261.5	279.5	360.2	–	0.82
PLA/PHB/S-0	246.9	306.5	244.7	272.1	327.3	358.6	5.18
PLA/PHB/S/8	264.4	311.1	261.6	278.3	356.2	–	2.62

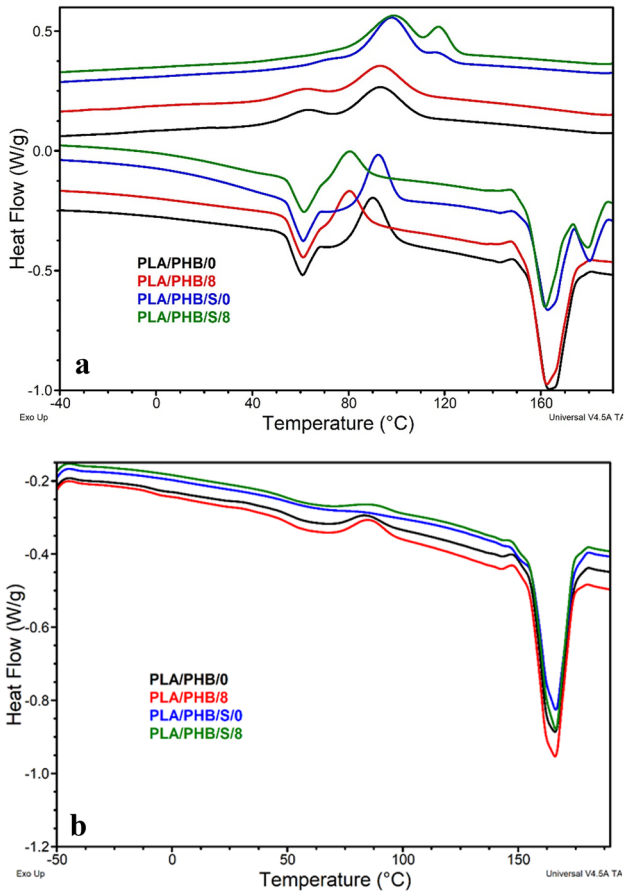

Fig. 6 **a** DSC thermograms corresponding to first heating run (bottom curve) and cooling (upper curve). **b** DSC curves obtained from the second heating run

PLA/cellulose composites [53, 54]. The residue was higher for the structured composites, as compared with PLA/PHB samples, as a result of the thermal decomposition of the silanized cellulose paper.

DSC Analysis

The DSC scans obtained from the first heating run show a single noticeable glass transition, between 55 and 57 °C, which is the T_g of the PLA, while for the PHB component this thermal event was not discernable (Fig. 6). The similar T_g values for the blend and structured-composite indicate that the mobility of the amorphous polymer chains was not hampered by the cellulose interlayer. The cold crystallization peak of PLA at around 90 °C in both samples, indicates that PHB crystals act as nucleating agents in PLA, which promote its recrystallization. This is consistent with previous research made on PLA/PHB blends, with the ratio of 75/25 [17, 18, 39]. However, a decrease of the T_{cc} with about 10 °C was observed after soil degradation (Table 4) showing faster crystallization. This may be a result of the biodegradation processes leading to a decrease of the molecular weight of PLA, also highlighted by FTIR.

A single endotherm corresponding to the melting of PLA/PHB blend was obtained before and after composting in both the first and the second heating cycles. On the contrary, a multi-melting process was observed for the PLA/PHB composites in the first heating cycle, similar to previous reports [39]. The melting peak at 161–163 °C corresponds to the melting of stable PLA α homocrystals developed during the heating process. The peak at 180 °C corresponds to the melting of the as-formed PHB crystals during the pressing process and recrystallized PHB crystals formed during DSC

Table 4 DSC parameters (glass transition temperature—T_g, melting temperature—T_m, enthalpy—ΔH, crystallization temperature—T_{cc})

Sample	First scan							Second scan	
	$T_{g,PLA}$ (°C)	$T_{cc,PLA}$ (°C)	ΔH_{cc} (J/g)	$T_{m,1}$ (°C)	$\Delta Hm_{,1}$ (J/g)	$T_{m,2}$ (°C)	$\Delta Hm_{,2}$ (J/g)	$T_{m,3}$ (°C)	$\Delta Hm_{,3}$ (J/g)
PLA/PHB/0	56.9	89.9	14.6	163.2	40.3	–	–	166.0	32.8
PLA/PHB/8	57.9	80.3	9.8	162.2	41.8	–	–	166.1	31.2
PLA/PHB/S/0	57.0	92.0	14.5	162.5	25.6	180.4	6.1	166.4	31.7
PLA/PHB/S/8	58.0	80.1	9.1	161.4	25.5	180.0	5.8	166.3	34.9

heating. This suggests the influence of cellulose interlayer in the formation of both polymer crystalline phases during the pressing process. A small crystallization peak was observed in all the samples just before the PLA's melting peak, during both the first and second heating run, which is ascribed to the presence of two crystal forms and recrystallization effects during heating [55]. This peak is less visible in the case of the samples after the soil burial tests, as expected, since are more vulnerable to biodegradation.

Dynamic Mechanical Analysis

The effect of the cellulose paper on the stiffness of the polymer blend sheets was investigated by DMA. Figure 7 shows the temperature dependence of the dynamic storage modulus and tan delta of the blend and structured composite before and after soil degradation and the corresponding data are listed in Table 5. The curves shape is typical for semi-crystalline polymers, with a high storage modulus in the glassy state followed by a dramatic decrease after the materials glass transition temperature. A consistent enhance in E′ was observed for the PLA/PHB/S/0 sample, which shows a strong reinforcing effect of the cellulose interlayer on the PLA/PHB matrix. The samples subjected to soil burial tests exhibited a decrease of the storage modulus in the glassy state (30 °C) of around 15% in the case of neat blend and 59% for the composite sample, as compared to unburied sample. The storage modulus drops significantly at the glass transition of the amorphous PLA (around 60 °C), but then increases, at 96 °C showing a peak, which indicates the recrystallization of PLA. This behavior is noticeable for all samples and is consistent with the work of Zhang & Thomas in the case of a PLA/PHB 75/25 blend [17]. The data also shows that cellulose layer did not hampered the recrystallization of PLA; on contrary, it started earlier, just above 80 °C (Fig. 7).

Table 5 E′ and tanδ of the PLA/PHB blend and sandwich composite before and after soil burial test

Sample name	Storage modulus (MPa)		Tanδ	
	30 °C	96 °C	Max value	T_g (°C)
PLA/PHB/0	4497	372	0.064	47.3
			1.886	68.5
PLA/PHB/8	3804	425	0.036	45.1
			0.524	69.1
PLA/PHB/S/0	7666	2392	0.138	73.1
PLA/PHB/S/8	3132	482	0.488	69.7

The decrease of the E′ upon aerobic degradation is associated with chain loss and decrease in molecular weight through a bulk hydrolysis. During first degradation stage the ester bonds are cleaved hydrolytically and fragmentation occurs. These small fragments are furthermore assimilated by microorganisms and fully mineralized to CO_2, H_2O and biomass. According to some authors the hydrolysis of PLA may be accelerated by the addition of hydrophilic fillers, which allows the penetration of the water molecules who initiate the degradation [55, 56]. Comparing the E′ values of the blend and composite before and after degradation we estimate that the addition of cellulose paper between two biopolymer layers increased the storage modulus but also the rate of PLA hydrolysis. Indeed, the E′ value of the composite became lower than that of the blend after composting.

A glass transition event was observed in all the samples at about 70 °C (Fig. 8) and corresponds to the glass transition of the PLA component. A small shoulder was observed at a lower temperature only in the PLA/PHB blend, before and after composting. This may be related to the glass transition of the PHB component which is in smaller amount in the blend and contain a large crystalline phase, therefore low

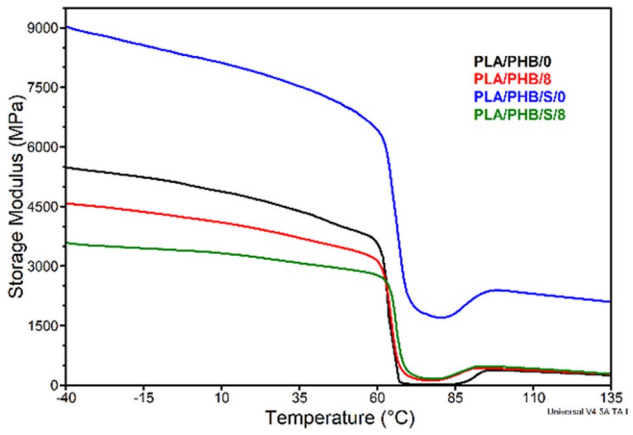

Fig. 7 Storage modulus (E′)

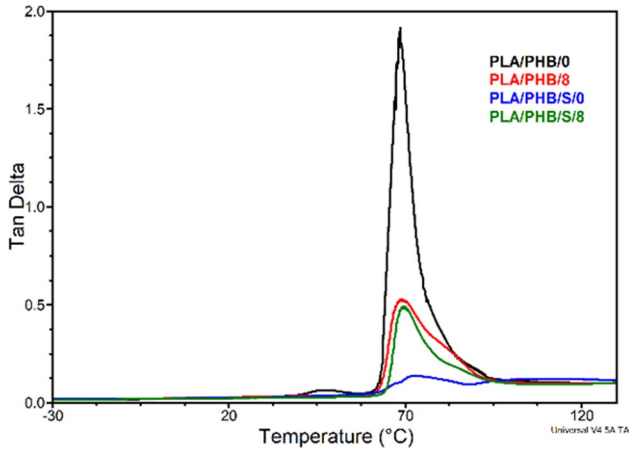

Fig. 8 tanδ curves for the samples before and after soil burial test

amorphous content. This shoulder was not observed in the composite sample, biodegraded or not, being probably an effect of the post processing by compression.

The damping factor (tan δ) at the glass transition temperature was high in the case of the original PLA/PHB blend and decreased after composting due to the physical and chemical changes induced by the soil degradation and highlighted by FTIR, SEM and XRD. The structured composite showed a much lower tan δ value due to the influence of cellulose paper and silanization which strongly decreased the polymers chains mobility and increased the stiffness. After the soil burial of the composite, the influence of moisture from the soil and different degradation processes favored by the presence of cellulose, led to the decrease of the molecular weight and increased chains mobility, increasing the damping.

Conclusions

We conducted biodegradation experiments on PLA/PHB blend and composite at ambient temperature, using cattle manure in the soil composition, to ensure an appropriate bacterial activity. These conditions better illustrate the real ones, since biopolymer based products are more likely to be disposed in environments characterized by the mesophilic content rather than high temperatures. The chemical changes of both neat and structured composite after 8 months in composting were consistent, as revealed by FTIR analysis. The XRD crystallinity of all the samples significantly increased during the soil burial test, which confirms that the material is in initial stage of degradation, where only the amorphous regions are degraded. Moreover, DSC measurements showed that the degradation of a PLA/PHB matrix occurs also at environmental temperatures, which confirm the morphological and X-ray analysis. The changes observed in the appearance and physico-chemical properties of the samples exposed to soil degradation at moderate temperature let us to conclude that both PLA/PHB and PLS/PHB/S will remain stable ensuring a short-time protection for humid foodstuff. However, both materials would degrade after a period of exposure to microorganisms and relative humidity. The results lead to the conclusion that a possible application of this type of material could be Tetrapak packaging for long packaging.

Acknowledgements This work was supported by the Ministry of Education and Research, Core Program, Contract No. 23N/2019, PN.19.23.02.01.07.

Compliance with Ethical Standards

Conflict of interest The authors declare that they have no competing interests.

References

1. Dhall RK, Alam MS (2020) Biodegradable packaging. Encyclopedia of renewable and sustainable materials. Elsevier, Amsterdam, p 26
2. Wang Y, Duo T, Xu X, Xiao Z, Xu A, Liu R, Jiang C, Lu J (2020) Eco-friendly high-performance poly(methyl methacrylate) film reinforced with methylcellulose. ACS Omega 5:24256–24261
3. Payne J, McKeown P, Jones M (2019) A circular economy approach to plastic waste. Polym Degrad Stab 165:170–181
4. Kumar S, Singh P, Gupta SK, Ali J, Baboota S (2020) Biodegradable and recyclable packaging materials: a step towards a greener future. Encyclopedia of renewable and sustainable materials. Elsevier, Amsterdam, p 328
5. Arrieta MP, Fortunati E, Dominici E, Rayón E, López J, Kenny JM (2014) Multifunctional PLA–PHB/cellulose nanocrystal films: processing, structural and thermal properties. Carbohydr Polym 107:16–24
6. Tharanathan RN (2003) Biodegradable films and composite coatings: past, present and future. Trends Food Sci Technol 14:71–78
7. Panaitescu DM, Frone AN, Chiulan I (2016) Nanostructured biocomposites from aliphatic polyesters and bacterial cellulose. Ind Crop Prod 93:251–266
8. Vasile C, Pamfil D, Râpă M, Darie-Niţă RN, Mitelut AC, Popa E, Popescu PA, Drăghici MC, Popa ME (2018) Study of the soil burial degradation of some PLA/CS biocomposites. Composites B 142:251–262
9. Södergård A, Stolt M (2002) Properties of lactic acid-based polymers and their correlation with composition. Prog Polym Sci 27:1123–1163
10. Siakeng R, Jawaid M, Asim M, Siengchin S (2020) Accelerated weathering and soil burial effect on biodegradability colour and texture of coir/pineapple leaf fibres/PLA biocomposites. Polymers 12:458–472
11. Mathew AP, Oksman K, Sain M (2005) Mechanical properties of biodegradable composites from poly lactic acid (PLA) and microcrystalline cellulose (MCC). J Appl Polym Sci 97:2014–2025
12. Fukushima K, Tabuani D, Kamino G (2009) Nanocomposites of PLA and PCL based on montmorillonite and sepiolite. Mater Sci Eng C 29:1433–1441
13. Pandey JK, Reddy KR, Kumar AP, Singh RP (2005) An overview on the degradability of polymer composites. Polym Degrad Stab 88:234–250
14. Liua Y, Zhab Z, Yeb H, Lina X, Yan Y, Zhang Y (2019) Accelerated biodegradation of PLA/PHB-blended nonwovens by a microbial community. RSC Adv 9:10386–10394
15. Panaitescu DM, Frone AN, Chiulan I (2017) Green composites with cellulose nanoreinforcements. In: Thakur VK, Thakur MK, Kessler MR (eds) Handbook of composites from renewable materials. Wiley, Hoboken, p 299
16. Abdelwahab MA, Flynn A, Chiou BS, Iman S, Orts W, Chiellini E (2012) Thermal, mechanical and morphological characterization of plasticized PLA-PHB blends. Polym Degrad Stab 97:1822–1828
17. Zhang M, Thomas NL (2011) Blending polylactic acid with polyhydroxybutyrate: The effect on thermal, mechanical, and biodegradation properties. Adv Polym Technol 30:67–79
18. Arrieta MP, López J, Hernández A, Rayón E (2014) Ternary PLA-PHB- Limonene blends intended for biodegradable food packaging applications. Eur Polym J 50:255–270
19. Navarro M, Ginebra MP, Planell JA, Barrias CC, Barbosa MA (2005) In vitro degradation behavior of a novel bioresorbable composite material based on PLA and a soluble CaP glass. Acta Biomater 1:411–419

20. Tokiwa Y, Calabia BP (2006) Biodegradability and biodegradation of poly(lactide). Appl Microbiol Biotechnol 72:244–251
21. Mehlika K, Alkan U (2019) Influence of time and room temperature on mechanical and thermal degradation of poly(lactic) acid. Therm Sci 23:383–390
22. Müller RJ (2005) Biodegradability of polymers: regulations and methods for testing. In: Steinbüchel A (ed) Biopolymers. Willey, New York
23. Xu A, Wang Y, Gao J, Wang J (2019) Facile fabrication of a homogeneous cellulose/polylactic acid composite film with improved biocompatibility, biodegradability and mechanical properties. Green Chem 21:4449–4456
24. Haider TP, Volker C, Kramm J, Landfester K, Wurm FR (2019) Plastics of the future? The impact of biodegradable polymers on the environment and on society. Angew Chem Int Ed 58:50–62
25. Bagheri AR, Laforsch C, Greiner A, Agarwal S (2017) Fate of so-called biodegradable polymers in seawater and freshwater. Glob Chall 1:1700048
26. Satti SM, Shah AA, Marsh TL, Auras R (2018) Biodegradation of poly(lactic acid) in soil microcosms at ambient temperature: evaluation of natural attenuation, bio-augmentation and bio-stimulation. J Polym Environ 26:3848–3857
27. Luo Y, Lin Z, Guo G (2019) Biodegradation assessment of poly (lactic acid) filled with functionalized titania nanoparticles (PLA/TiO_2) under compost conditions. Nanoscale Res Lett 14:56
28. Sinha Ray S, Yamada K, Okamoto M, Ueda K (2003) New polylactide-layered silicate nanocomposites. 2. Concurrent improvements of material properties, biodegradability and melt rheology. Polymer 44:857–866
29. Gois GDS, Andrade MFD, Garcia SMS, Vinhas GM, Santos ASF, Madeiros ES, Olivieara JE, Almeida YM (2017) Soil biodegradation of PLA/CNW nanocomposites modified with ethylene oxide derivatives. Mater Res 20:899–904
30. Lertphirun K, Srikulkit K (2019) Properties of poly (lactic acid) filled with hydrophobic cellulose/SiO composites. Int J Polym Sci 2019:7835172
31. Cyras VP, Soledad CM, Analia V (2009) Biocomposites based on renewable resource: acetylated and nonacetylated cellulose cardboard coated with polyhydroxybutyrate. Polymer 50:6274–6280
32. Wei L, Liang S, McDonald AG (2015) Thermophysical properties and biodegradation behavior of green composites made from polyhydroxybutyrate and potato peel waste fermentation residue. Ind Crops Prod 69:91–103
33. Fortunati E, Armentano I, Iannoni A, Barbale M, Zaccheo S, Scavone M, Visai L, Kenny JM (2012) New multifunctional poly(lactide acid) composites: mechanical, antibacterial, and degradation properties. J Appl Polym Sci 124:87–98
34. Yaacob ND, Ismail H, Sam ST (2016) Soil burial of polylactic acid/paddy straw powder biocomposite. BioResources 11:1255–1269
35. Phetwarotai W, Potiyaraj P, Aht-Ong D (2013) Biodegradation of polylactide and gelatinized starch blend films under controlled soil burial conditions. J Polym Environ 21:95–107
36. Woolnough CA, Yee LH, Charlton T, Foster LJR (2010) Environmental degradation and biofouling of 'green' plastics including short and medium chain length polyhydroxyalkanoates. Polym Int 59:658–667
37. Rudnik E, Briassoulis D (2011) Degradation behavior of poly(lactic acid) films and fibres in soil under Mediterranean field conditions and laboratory simulations testing. Ind Crops Prod 33:648–658
38. Rudnik E (2019) Biodegradability testing of compostable polymer materials under laboratory conditions. In: Rudnik E (ed) Compostable polymer materials, 2nd edn. Elsevier, Boston, pp 163–237
39. Frone AN, Panaitescu DM, Chiulan I, Gabor AR, Nicolae CA, Oprea M, Ghiurea M, Gavrilescu D, Puitel AC (2019) Thermal and mechanical behavior of biodegradable polyester films containing cellulose nanofibers. J Therm Anal Calorim 138:2387–2398
40. Panaitescu DM, Nicolae CA, Frone AN, Chiulan I, Stanescu PO, Draghici C, Iorga M, Mihailescu M (2017) Plasticized poly(3-hydroxybutyrate) with improved melt processing and balanced properties. J Appl Polym Sci 134:44810
41. Hong SG, Hsu HW, Ye MT (2013) Thermal properties and applications of low molecular weight polyhydroxybutyrate. J Therm Anal Calorim 111:1243–1250
42. Vey E, Rodger C, Booth J, Claybourn M, Miller AF, Saiani A (2011) Degradation kinetics of poly(lactic-co-glycolic) acid block copolymer cast films in phosphate buffer solution as revealed by infrared and Raman spectroscopies. Polym Degrad Stab 96:1882–1889
43. Rapa M, Nita RND, Vasile C (2017) Influence of plasticizers over some physico-chemical properties of PLA. Mater Plast 54:73–78
44. Fukushima K, Abbate C, Tabuani D, Gennari M, Camino G (2009) Biodegradation of poly(lactic acid) and its nanocomposites. Polym Degrad Stab 94:1646–1655
45. Guo L, Sato H, Hashimoto T, Ozaki Y (2010) FTIR study on hydrogen-bonding interactions in biodegradable polymer blends of poly(3-hydroxybutyrate) and poly(4-vinylphenol). Macromolecules 43:3897–3902
46. Arrieta MP, Fortunati E, Dominici F, Rayón E, López J, Kenny JM (2014) PLA-PHB/cellulose based films: mechanical, barrier and disintegration properties. Polym Degrad Stab 107:139–149
47. Khabbaz F, Karlsson S, Albertsson AC (2000) PY-GC/MS an effective technique to characterizing of degradation mechanism of poly (L-lactide) in the different environment. J Appl Polym Sci 78:2369–3237
48. Chiulan I, Panaitescu DM, Frone AN, Teodorescu M, Nicolae CA, Căşărică A, Tofan V, Sălăgeanu A (2016) Biocompatible polyhydroxyalkanoates/bacterial cellulose composites: preparation, characterization, and in vitro evaluation. J Biomed Mater Res A 104:2576–2584
49. Panaitescu DM, Frone AN, Chiulan I, Gabor RA, Spătaru IC, Căşărică A (2017) Biocomposites from polylactic acid and bacterial cellulose nanofibers obtained by mechanical treatment. BioResources 12:662–672
50. Guo P, Wang F, Duo T, Xiao Z, Xu A, Liu R, Jiang C (2020) Facile fabrication of methylcellulose/PLA membrane with improved properties. Coatings 10(5):499
51. Altaee N, El-Hiti GA, Fahdil A, Sudesh K, Yousif A (2016) Biodegradation of different formulations of polyhydroxybutyrate films in soil. SpringerPlus 5:762–762
52. Radha KV, Saranya S (2019) Polyhydroxybutyrate-based nanoparticles for controlled drug delivery. In: Munmaya KM (ed) Applications of encapsulation and controlled release. CRC Press, Boca Raton
53. Kowalczyk M, Piorkowska E, Kulpinski P, Pracella M (2011) Mechanical and thermal properties of PLA composites with cellulose nanofibers and standard size fibers. Composites A 42:1509–1514
54. Monticelli O, Bocchini S, Gardella L, Cavallo D, Cebe P, Germelli G (2013) Impact of synthetic talc on PLLA electrospun fibers. Eur Polym J 49:2572–2583
55. Stloukal P, Pekařová S, Kalendova A, Mattausch H, Laske S, Holzer C, Chitu L, Bodner S, Maier G, Slouf M, Koutny M (2015) Kinetics and mechanism of the biodegradation of PLA/clay nanocomposites during thermophilic phase of composting process. Waste Manage 42:31–40
56. Sun C, Huang Z, Liu Y, Li C, Tan H, Zhang Y (2020) The effect of carbodiimide on the stability of wood fiber/poly(lactic acid) composites during soil degradation. J Polym Environ 28:1315–1325